

A Novel Compact and Lightweight Actuator for Wearable Robots

Massimo Bergamasco, Fabio Salsedo, Simone Marcheschi, Nicola Lucchesi and Marco Fontana

Abstract— Advanced robotics needs a new breed of actuators, capable to exhibit a large number of desirable features, ranging from high power/torque density, high efficiency, zero backlash and low noise, to low reflected mechanical impedance, high bandwidth and accuracy. Even if it is quite evident that to fully match these requirements new basic actuation principles have to be investigated and developed in the long term, there is still scope now for innovating the field by combining mature components into new actuation schemes. This paper reports the development and the experimental evaluation of a new actuator, aiming at improving the torque density and the mechanical efficiency. The device has shown impressive performances being able to exert up to 500Nm continuous torque and 800Nm peak torque with 85% mechanical efficiency and zero backlash, up to 60°/s maximum output speed for a total weight of just 6Kg, comprising the structural case covering the internal mechanics. The actuator has been expressly conceived as an actuation module to be integrated in a fully powered whole body exoskeleton intended for material handling in tight and unstructured environments (see Fig.1).

I. INTRODUCTION

WITH advanced robotics it is generally indicated the set of those envisaged robotic systems that in the future will be able to operate outside the working cells, where the present industrial robots are confined, i.e. in direct and tight interaction with unstructured environments and, in particular and more challenging, with humans.

According to some robotic researchers and also leaders of industrial robots manufacturing companies, due to the impressive progresses in the field of computing power, embedded electronics, communication and sensing technology and control algorithms we are very close to the moment on which this vision will turn in reality [1].

Yet, the presently available actuation technology can seriously hinder the widespread and successful introduction of advanced robotics in the society, due to the less than ideal features/performances exhibited by the commonly used actuation solutions, ranging from the low torque/power density, low efficiency, high friction, backlash and noise, to high reflected mechanical impedance, low bandwidth and accuracy. The comparison of those performances with the corresponding ones of the natural muscles of animals makes

Manuscript received September 15, 2009. This work was supported in part by the Italian Ministry of Defense under National Research Project PRN 266.

All the authors are from PERCRO Lab of Scuola Superiore S. Anna, Pisa, Italy (www.percro.org).

Massimo Bergamasco acts as contact author (phone: + 39 050 883786; fax: +39- 050- 883333; e-mail: massimo.bergamasco@sss.up.it).



Fig. 1. The fully actuated body extender developed at PERCRO

clear the need for a long term investigation and development of new basic actuation principles (such as the Electro Active Polymers, see for example [2]), that, indeed, is on the way by some decades on, even if at present it has not produced components reliable enough to be used in full time working robots. However, there is still scope for innovating now the field by combining mature components into innovative actuation schemes. This is clearly demonstrated by, for example, a wealth of recent researches that, using conventional electric motors in combination with passive elastic elements purposely introduced in the mechanical transmission, allowed to achieve significant improvements of the force control accuracy, the energy efficiency in the execution of specific tasks, the bandwidth of the force control, the shock tolerance and the safety in case of collision of the robotic links with humans (see [3] for a comprehensive survey of these researches).

Yet, the goal of improving other performances such as the torque density and mechanical efficiency has been poorly addressed. Enhancing these performances is central for the development of wearable robots, such as active orthoses, prosthesis and body extenders. Indeed more compact actuators allow to reduce the mass of the device and the energy requirements and also to improve its aesthetic and hence the user acceptability, while higher mechanical efficiency and back-drivability allow a sufficiently accurate sensor less estimation of the interaction forces of the device with the external environment

Contributing to the fulfillment of this need, the Perceptual Robotics Laboratory has developed and tested a new actuation module that combines into an innovative scheme mature actuation components.

II. BACKGROUND

Among conventional actuation solutions, pneumatic and hydraulic cylinders exhibit the highest force/power to weight ratios and force to volume ratios. However, they are characterized by non linearity, stiction, and compliance that can cause instabilities in high performance closed loop force control. Firstly introduced in 1960, the McKibben Muscles, not having internal moving parts that require rubbing sealing, exhibit lower stiction but they still present significant hysteresis in the force-length characteristic due to the static friction occurring among the helical woven fibers [4]. Moreover, as for all the fluidic actuators, their functioning requires a number of other complementary components, such as pumps, servo-valves, filters, accumulators, manifolds, pipes, that are costly, noisy and difficult to maintain.

In consideration of the discussed drawbacks of the pneumatic and hydraulic actuators, the electric motors have been elected as the preferred technology for the actuation of the robotic joints. Indeed, they exhibit many desirable features, like high bandwidth, linearity, accuracy, stiffness, efficiency and low friction and maintenance costs. Unfortunately, the torque density achievable with the present technology of electromagnetic motors is unsuitable for realizing light-weight and compact robots. Significant improvements of the torque density can be achieved stressing some motor design parameters, like the number of poles, the stator to rotor air gap or changing the geometry of the magnetic engagement or providing water cooling, but at present they are not enough for matching the requirements of the most demanding applications (see for example [5] in which a new brushless torque motor with 10Nm/Kg torque density has been developed). To overcome the problem, high reduction ratio speed reducers are used in combination with the electric motors, even if the features of the resulting actuators are seriously deteriorated due to the friction, backlash, elasticity, transmission ripple introduced by these components. The integrated joint developed at DLR [6], using last generation Harmonic Drive speed reducers (HD) with reduction ratio of the order of 100 in combination with high performance DC torque motors, can be considered the state of art of this kind of solution. It allows to achieve good level of torque density, but the back drivability is less than ideal due to the relatively low mechanical efficiency, that is also variable with temperature, speed and torque (see for example the technical data of a high quality HD reported in [7]). An interesting alternative to produce a high reduction ratio is proposed in [8], in which an electric motor drives a hydraulic volumetric pump supplying oil flow to a hydraulic volumetric motor. High transmission reductions can be simply achieved acting on the ratio between the pump piston

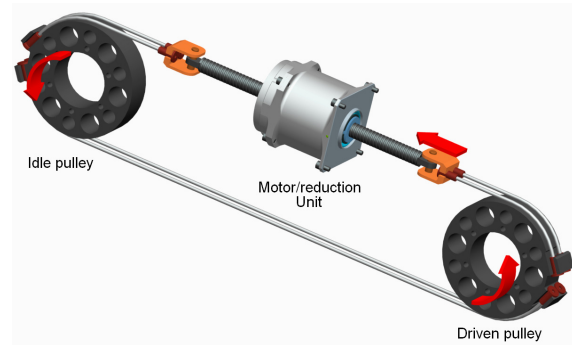


Fig. 2. Actuation scheme proposed in [9] (simplified).

active surface and that of the motor. However the static friction generated by the rubbing sealing between the piston and the cylinder of the pump is also amplified on the output axis. In [9] a lead screw is used as main speed reducer in combination with two metallic tendons and a driven and an idle pulleys to convert the linear motion into a rotation on the output axis (see the simplified scheme of Fig. 2). The scheme is potentially interesting if a ball lead screw is used, by virtue of its beneficial features in terms of high reduction ratio, lightness, zero backlash, smoothness and high mechanical efficiency that are not affected by the metallic tendon transmission. Furthermore it introduces elastic elements in the transmission that can reduce the peak forces occurring on the transmission components during possible collisions of the robotic limb with the external environment. Yet, it has the big drawback of producing large encumbrances in case large angular strokes and torques are required. Furthermore guiding elements are needed to prevent the rotation of the screw around its axis.

III. BASIC ACTUATION SCHEME

As anticipated, the new actuation scheme has been expressly conceived for driving the joints of a whole body exoskeleton intended for material handling. The following main system requirements have been set as a starting point to the mechanical design of the robotic limbs of the device:

- kinematics isomorphic to that of the human limbs, i.e. mechanical axes substantially aligned with the corresponding axes of the physiological joint, to keep at minimum the joint torque requirements when covering large portion of the natural workspace of the human limbs;
- actuation achieved through electric motors, to ensure better control accuracy, simpler system maintenance and better user's safety;
- encumbrance of the mechanics adherent to that of the human limbs, to allow the operator to intuitively control the posture of the device avoiding the occurring of interferences of the structure with the surrounding environment, when operating in tight spaces;
- mechanics of the robotic limbs conceived as a series of self contained 1 DoF actuation modules connected

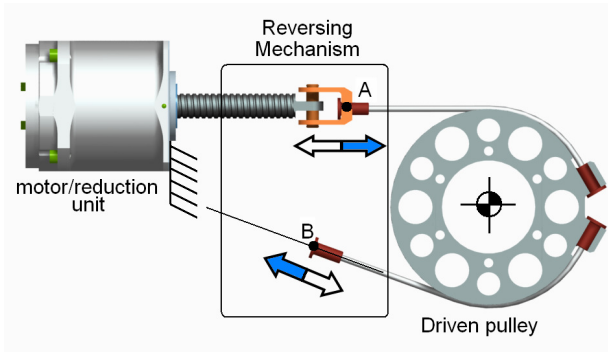


Fig. 3. Conceptual scheme of the new actuator.

together to form a serial chain, each module providing actuation, sensing, structural and electronic (sensor acquisition, motor current supply and serial communication) functionalities, to achieve as much as possible a modular design that could reduce the cost of the system.

On the basis of these requirements two kinds of actuation modules have been distinguished:

- 1) **transversal joints**, having their major encumbrance direction aligned with the major dimension of the human limb and the axis of the actuated joint orthogonal to that direction (for example the elbow flexion-extension joint);
- 2) **longitudinal joints**, having their encumbrance equally distributed around the actuated axis that is aligned with the major dimension of the human limb (for example the forearm pronosupination joint).

That said, the new actuation scheme has been conceived for the implementation of the transversal joint, and in particular for those requiring a relatively large angular stroke and output torque. For these joints, the ideal encumbrance distribution should have a major dimension in the direction orthogonal to the actuated axis, while the other two, and in particular the one aligned with the output axis, should be as small as possible, to keep the mechanics more adherent to the human limb. The solution of using an electric motor in combination with a geared speed reducer mounted coaxially with the output axis, is poorly suitable because produces relatively large axial and radial encumbrance.

These considerations together with the general requirement of reducing the weight of the actuation module led us to select the ball lead screw as the main speed reducer. Indeed, this component has many beneficial features, such as a high mechanical efficiency, zero backlash, smooth operation, low noise and low encumbrance, mass and inertia. Furthermore it allows to position the axis of the motor orthogonally to the output axis and, hence, to have an encumbrance compatible with the requirement of the transversal joint.

To have a rotational output, a mechanism is required to convert the linear motion of the screw. This can be simply achieved by directly connecting the screw to the output link, but in the case of large required output angular strokes an unacceptable reduction of the maximum generable torque

near the angular limits is produced. One simple solution to keep constant the distance of the lead screw force action line from the output axis and hence the maximum generable torque is to use a metallic tendon connected to the endpoint of the screw and wrapped to a driven pulley, as proposed in [9]. This is preferable with respect to other solutions, such as rack-pinion transmission, because it has better mechanical efficiency, does not introduce backlash and does not produce forces with components orthogonal to the axis of the screw. Furthermore it introduces some compliance in the transmission that is useful to reduce peak forces during collisions with external rigid environments.

However, to generate bidirectional torques (clockwise and counterclockwise), two metallic tendons must be used. The second tendon can be driven as proposed in [9], but this solution produces very large encumbrance in the orthogonal direction. Indeed, indicating with Θ , R and H , respectively the angular stroke, the radius of the driven pulley and the axial dimension of the motor, the minimum theoretical encumbrance L is:

$$L = 2\Theta R + 2R + H = 2R(\Theta + 1) + H$$

For a given maximum axial force generable by the motor reduction unit, higher required angular strokes and output torques produce higher actuator encumbrances.

To drastically decrease this drawback, we propose a new actuation scheme (see Fig. 3), that envisages the use of a mechanism, located between the motor reduction unit and the driven pulley, to drive the second tendon, in such a way that, if the endpoint A of the first tendon moves by a quantity along a line tangent to the primitive of the driven pulley, the endpoint B of the second tendon moves by the same quantity in the opposite direction, along a second line that is tangent to the same primitive. This kinematical property ensures that the total length of the tendon circuit (from A to B) remains constant for the different output angular positions of the driven pulley. This implies that also any given tendon preload remains constant. According to this scheme the theoretical minimum encumbrance is:

$$L = \Theta R + R + H = R(\Theta + 1) + H$$

that is quite half the encumbrance of the previous scheme. It is worth noting that, in general, the second line along

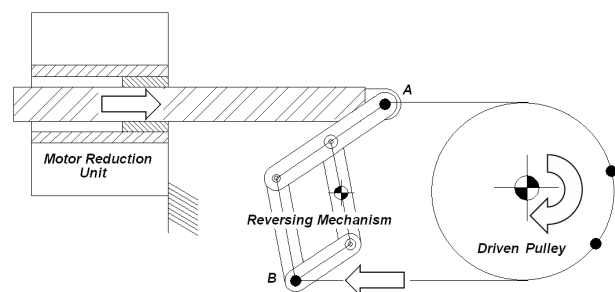


Fig. 4. First embodiment of the reversing mechanism.

which point B moves, can be inclined with respect the screw axis. This is useful for reducing the transversal encumbrance of the actuation module and increasing the angular stroke beyond 180°.

IV. EMBODIEMENTS OF THE REVERSING MECHANISM

Three different embodiments have been identified for the implementation of the reversing mechanism envisaged in the new actuator scheme.

The first embodiment envisages the use of a pantograph mechanism for reversing the motion of the end point of the screw (see Fig. 4). Referring to Fig. 5, only the axis of rotational pair O is fixed, while the other axes are moving. To ensure the required kinematics property for the reversing mechanism, the following geometric conditions must be satisfied:

$$OC = OD, CA = DB, AE = CD, ED = AC$$

The last 2 conditions ensure that the quadrilateral ACDE is a parallelogram and hence BE is parallel to AC and the angles \widehat{ACO} and \widehat{ODB} are equal. Together with the first two conditions this ensures that the triangles OCA and ODB are equal and hence also Y_a and Y_b are equal. In conclusion if Y_a varies of the quantity ΔY , Y_b varies of the same quantity but in the opposite direction. More in general the points A, O and B lie on line and it is always $OA=OB$. Hence if point A (or B) follows a planar trajectory, B (A) follows the same trajectory but rotated of 180° around the fixed point O. In particular if point A moves along a straight line, point B moves along another straight line, resulting the rotation by 180° of the first line around the fixed point O.

By applying the virtual work principle it can be easily demonstrated that, in the case of negligible friction in the rotational pairs, if a force vector is applied in point A (or B), point B (A) generates to the external world a force vector that is equal to the force vector applied in A (B) and rotated of 180° around the fixed point O. In particular if A moves along a straight line, then also B moves along a straight line and if the force applied in B has null component in the direction normal to its straight line, then point A transfers to the external work a force with a null component in the direction normal to its straight line. Applied to the case of

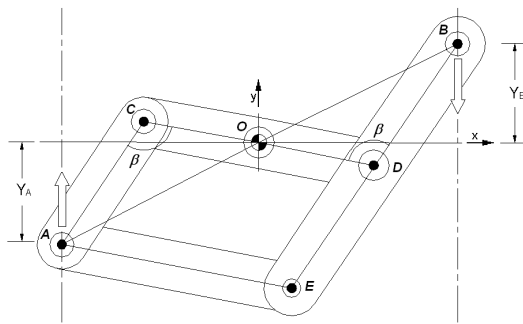


Fig. 5. Geometry of the pantograph mechanism.

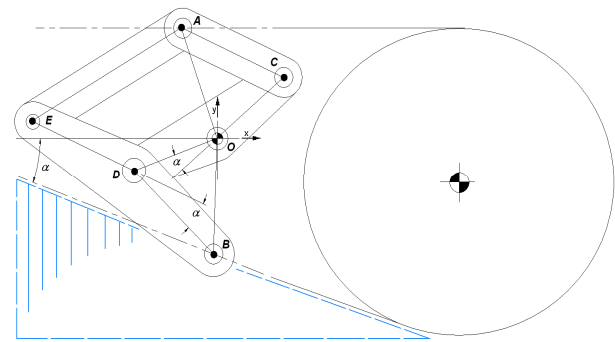


Fig. 6. Variant of the pantograph mechanism.

our actuation scheme, this property ensures that the screw is not loaded with force having component normal to its axis. Indeed, if the straight line followed by point B, when point A moves along the axis of the screw, is tangent to the primitive of the driven pulley, then, due to bending flexibility of the metallic tendon, the force applied by the tendon in B will have a negligible component normal to the straight line and hence this will produce a negligible force component normal to the axis of the screw.

An interesting variant of this mechanism exhibits the same properties described above but rotating trajectories and forces by an angle different from 180° (see Fig. 6). This can be easily achieved inserting an angle (α) between the 2 segments OC and OD of the lever rotating around O, while always satisfying the same above geometric conditions. As anticipated this is convenient for reducing the transversal encumbrance and increasing the angular stroke.

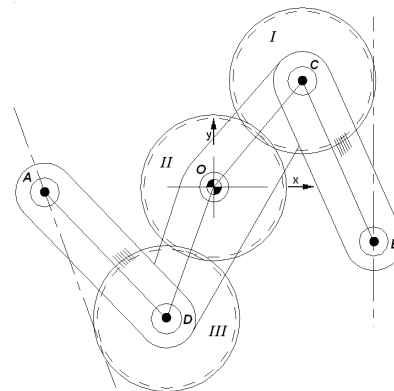


Fig. 7. Second embodiment of the reversing mechanism.

The second embodiment uses gears instead of the parallelogram to mirror the angles \widehat{OCB} and \widehat{ODA} (see Fig. 7). Gear I and gear III have equal radius and are integral, respectively to lever CB and lever DA, while gear II is idle around fixed axis O. Also this embodiment can produce rotations of the trajectories and forces different from 180°. It is worth to note that any backlash existing in the engagement of the gears can be canceled by a suitable preload on the two tendons.

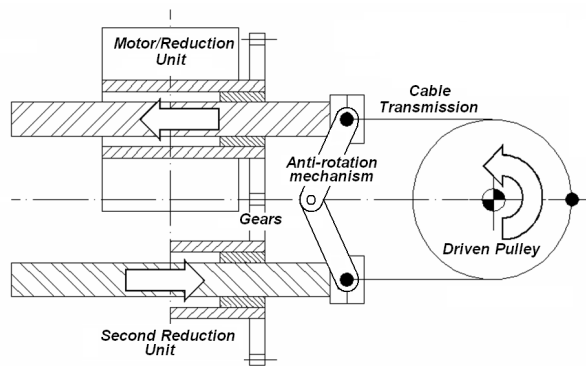


Fig. 8. Third embodiment of the reversing mechanism.

The third embodiment is somewhat different from the previous ones because the reversion of the motion is generated directly from the rotation of the motor, using a second lead screw whose nut is brought in rotation by a couple of gears with equal radius (see Fig. 8). Also in this case any backlash existing in the gears can be cancelled by a suitable preload in the tendons. To prevent the rotation of the screw around their axes, the end points of the screws have been connected together with a two link mechanism, having three rotational pairs of which two in correspondence of the endpoints of the screws and one for the relative articulation of the links.

Even if in principle this embodiment could have a variant that allows the introduction of an angle between the two axes of the screws, in practice the implementation could be complex due to the need to use bevel gears and to possible interferences of the second screw with the actuator's body.

V. DEVELOPMENT OF THE ACTUATION MODULE

The first embodiment has been selected for the following detailed design phase of the new actuation module. It has been preferred to the second embodiment due to the lighter implementation of the angle mirroring (angles \widehat{OCB} and \widehat{ODA} , see point IV) allowed by the parallelogram compared to that using the gears. Furthermore in this embodiment only two levers are loaded with bending stress, while in the second embodiment they are three. Finally it has been estimated that the second embodiment would have produced a higher total friction, due to the gear engagement. The third

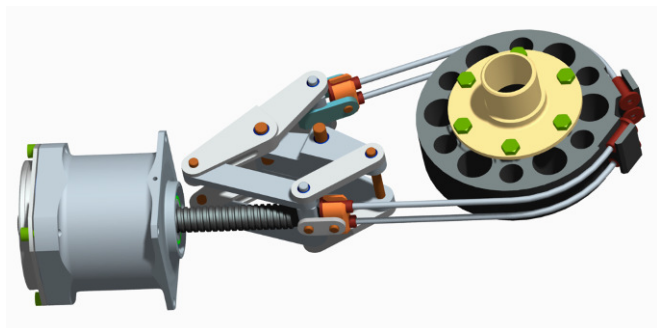


Fig. 9. CAD view of the actuation module (without case).

embodiment has not been selected, due to the anticipated implementation difficulties in inserting an angle between the two screw axes.

The actuation module has been designed for delivering a maximum output continuous torque of about 500Nm at a maximum output speed of 60°/s for an angular stroke of 110°. Due to the general requirement to reduce the total mass of the actuation module the mechanics of the motor/reduction unit has been expressly designed and optimized for the application. The core components of the unit (the electric motor and the lead screw) have been selected among the best commercially available. In particular a frameless brushed DC torque motor with rare earth permanent magnet manufactured by AXYIS Technology Inc. USA and a 12mm diameter, 4mm lead precision ball screw manufactured by THK CO. LTD, Japan have been selected.



Fig. 10. The integrated actuation module.

The torque motor is able to deliver up to 4.5-5.5Nm continuous torque depending on the thermal resistance from the winding to the environment and more that 7Nm peak torque at a maximum speed of 1050 rpm, weighting only 1.4 Kg (stator + rotor). The ball screw has been specified for delivering thrust forces up to 12000N and weights only 300g. A purposely developed incremental encoder with 1000 pulses/revolution has been integrated in the mechanics. The total mass of the motor reduction units is 2.4Kg and is able to deliver up to 8000N of continuous thrust force. The lever of the pantograph has been realized in high strength stainless steel (AISI 630 precipitation hardening stainless steel), while for the rotational pairs stainless steel axles and metallic plain bearings have been used. The 4mm metallic tendons with clamped terminals have been supplied by Carl Stahl GmbH, Germany, according to the required length, and can be pre-tensioned acting on a screw located between the part holding the tendon terminals and the output pin of the pantograph. The pretension can be registered to simply null the backlash (in this case a light value is sufficient) or to increase the stiffness of the transmission making the two tendons collaborate to the transmission of the torque (a higher value is needed in this case). The driven pulley, realized in hard anodized 7075-T6 aluminum with a set of slots to reduce the mass, has a primitive radius of 65mm, setting the total

TABLE I
COMPARISON OF THE NEW ACTUATOR PERFORMANCES
WITH THOSE OF THE BEST COMMERCIAL ACTUATORS

Model	PERCRO	Harmonic Drive AG CHA 50A	Exlar Corp. SLG 115	Schunk PRL 120
Nominal torque	520 Nm	456 Nm	283 Nm	216 Nm
Peak torque	610 Nm	980 Nm	288 Nm	372 Nm
Output speed	10 rpm	35 rpm	30 rpm	4,166 rpm
Output inertia	8,6 Kgm ²	26 Kgm ²	4 Kgm ²	--
Reduction	102	100	100	596
Backlash	Zero	Zero	10 Arc min.	Zero
Efficiency	85 %	--	86 %	--
Weight	6 Kg	19,9 Kg	15,4 Kg	3,6 Kg
Size	370x140x70 mm	222x222x189 mm	115x115x296 mm	132x132x156 mm
Nominal voltage	90 VDC	430 Vrms	115 Vrms	24 VDC

reduction ratio at 102. It rotates on two ball bearings and is directly flanged to the output actuator's output link. All the mechanics, apart the motor body, is contained in case made in casting aluminum, that provides structural strength for both the internal and external forces acting on the actuation module. The resulting CAD assembly model is depicted in Fig. 9. The total weight of the module is about 6Kg and it is contained in an encumbrance envelope of about 370x140x70mm. A picture of the integrated module with the boxes containing the electronics is reported in Fig. 10.

In Table 1, the main performances of the new actuation module are compared with those of the best actuators available on the market.

It is worth noting that the encumbrances of the commercial actuators can be approximated to a cylinder with axis aligned with the output axis and, hence, are not ideally distributed

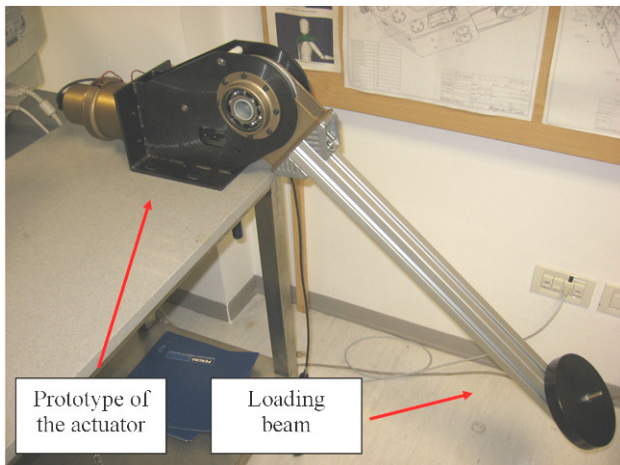


Fig. 11. Mechanical testbed.

for implementing a transversal joint. Furthermore, they require relatively long additional structural parts to connect the adjacent joints, while using the new actuation modules only short links are needed to complete the robotic structure. Indeed, the case covering the internal mechanics of the actuation module can be considered as a thin wall beam extending from one joint to the next and, hence, it is well suited to serve as a stiff structural part.

VI. EXPERIMENTAL TESTS

For investigating the performance of the novel actuator, an experimental prototype has been realized, having the same core components described in section V but a case with a simplified geometry. Furthermore, a loading beam has been connected to the driven pulley (see Fig. 11). To drive the motor, a PWM analog servo amplifier (Elmo Violin 10/100) has been used. The control of the testbed has been achieved using a DSpace 1103. Firstly, to evaluate the no load friction and motor torque ripple, the motor has been commanded to move at a constant speed of 30 degrees/sec using a PD position controller. The test allowed to estimate a motor torque ripple of about 0.22Nm (peak to peak) and an average dynamic friction of about 0.15Nm.

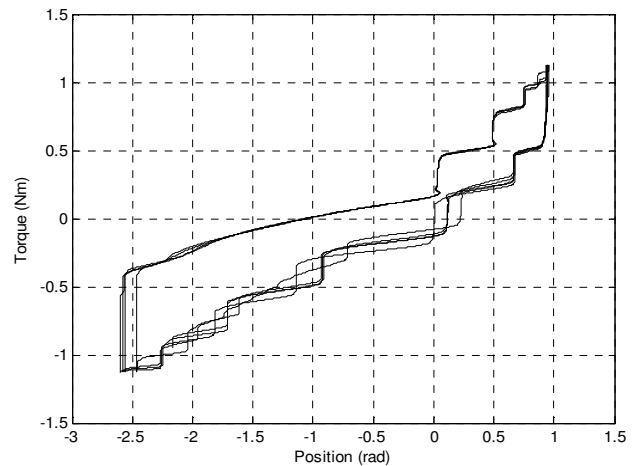


Fig. 12. Motor torque vs motor position with blocked motor shaft.

To evaluate the output actuator stiffness, the driven pulley has been mechanically blocked to the testbed frame and the motor has been controlled to generate a sinusoidal torque of 1.12Nm and 0.1Hz frequency. The motor shaft positions and the correspondent motor torques have been recorded. In Fig. 12, the recorded data for 4 different loading cycles are reported. In the case the screw force is transmitted through only the cable (positive values of torque in Fig. 12), the output stiffness is about 10400Nm/rad, while it decreases to about 5100Nm/rad when the force transmission is achieved through the cable and the pantograph. The discontinuities and the hysteresis shown by the graph are due to the stick slip phenomena in the mechanical transmission and to the breakaway torque of the motor.

VII. CONCLUSION

A new actuation scheme using mature components has been proposed and a self contained actuation module providing actuation, sensing structural and electronic functionalities has been developed according to it. The module has a very high torque density of the order of 80Nm/Kg due to a combination of a state of art torque DC torque motor with a very lightweight speed reducer consisting of a ball screw, a reversing mechanism, a driven pulley and two metallic tendons. The mechanical efficiency is also interesting being more than 85%, even if the total reduction ratio is more than 100. Furthermore the backlash is zero and the functioning is smooth and with low noise, due to the lack of continuous shocks during gear engagement. Moreover the scheme introduces a compliance in the force transmission that reduces the peak forces during the collision with the external environment. Future works will investigate the possibility to modify the actuation scheme and related control strategies in order to encompass also these beneficial features. A patent application has been submitted to the Italian patent office [10].

ACKNOWLEDGMENT

This work is partially funded by the Italian Ministry of Defense, in the framework of the national plan for the military research.

REFERENCES

- [1] A. Albu-Schaffer, O. Eiberger, M. Grebenstein, S. Haddadin, C. Ott, T. Wimbock, S. Wolf, G. Hirzinger, "Soft robotics", IEEE Robotics & Automation Magazine, vol.15, no.3, pp.20-30, September 2008
- [2] I.W. Hunter, S. Lafontaine, "A comparison of muscle with artificial actuators", IEEE Solid-State Sensor and Actuator Workshop, 1992. 5th Technical Digest., vol., no., pp.178-185, 22-25 Jun 1992
- [3] R. Ham, T. Sugar, B. Vanderborght, K. Hollander, D. Lefeber, "Compliant actuator designs", IEEE Robotics & Automation Magazine, vol.16, no.3, pp.81-94, September 2009
- [4] Ching-Ping Chou, B. Hannaford, "Measurement and modeling of McKibben pneumatic artificial muscles", IEEE Transactions on Robotics and Automation, vol.12, no.1, pp.90-102, Feb 1996
- [5] J. Hollerbach, I. Hunter, J. Lang, S. Umans, R. Sepe, E. Vaaler, I. Garabieta, "The McGill/MIT direct drive motor project", IEEE International Conference on Robotics and Automation, 1993, pp.611-617, vol.2, 2-6 May 1993
- [6] G. Hirzinger, N. Sporer, M. Schedl, J. Butterfass, M. Grebenstein, "Torque-Controlled Lightweight Arms and Articulated Hands: Do We Reach Technological Limits Now?", The International Journal of Robotics Research, Vol. 23, No. 4-5, 331-340 (2004)
- [7] *CPU-M Series - Technical Data*, Harmonic Drive AG, Limburg/Lahn, Germany, 2009. Available: <http://www.harmonic-drive.de/english/products/units/cpu-m/product-documentations.html>
- [8] H. Kaminaga, J. Ono, Y. Nakashima, Y. Nakamura, "Development of backdrivable hydraulic joint mechanism for knee joint of humanoid robots", IEEE International Conference on Robotics and Automation, ICRA '09, pp.1577-1582, 12-17 May 2009
- [9] P. Garrec, J.-P. Martins, F. Gravez, Y. Measson, Y. Perrot, "A New Force-Feedback, Morphologically Inspired Portable Exoskeleton" IEEE International Symposium on Robot and Human Interactive Communication, ROMAN 2006, pp.674-679, 6-8 Sept. 2006
- [10] "Attuatore compatto e leggero a escursione angolare limitata e elevata coppia" Italian Patent Application n. B10_0498, file April 30, 2008

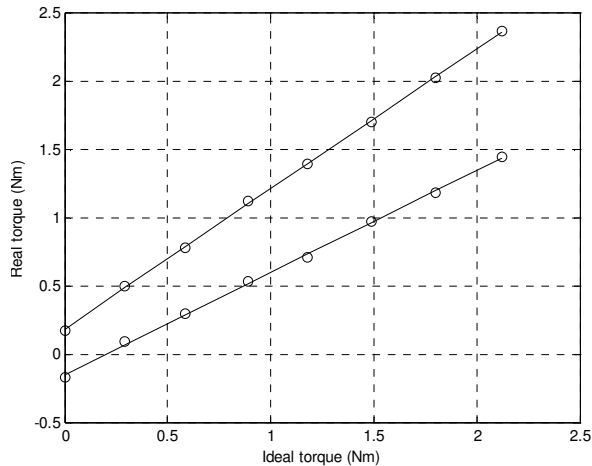


Fig. 13. Direct and reverse motion torque characteristic.

The efficiency of the actuator has been evaluated by recording the motor torque required for moving different known loads (up to 35Kg), applied at the extremity of the loading beam. For each load, both direct and reverse motions have been recorded. In Fig. 13, the measured motor torque versus the ideal torque (efficiency = 1) for different applied loads are reported. Direct and inverse efficiency have been estimated using the slope of two fitting straight lines, resulting in 86% and 84% respectively.

To investigate the dynamical performances of the actuator, a 2Nm amplitude Chirp Signal has been applied as motor torque in the range of frequency from 1Hz to 40Hz. Three tests with different masses have been carried out recording the motor position and the correspondent motor torque. Then, the acquired data have been post-processed for estimating the force to position frequency response. In Fig. 14, the Bode diagrams relative 5Kg, 10Kg and 15Kg show zeros at 6Hz, 5Hz and 4.5Hz respectively.

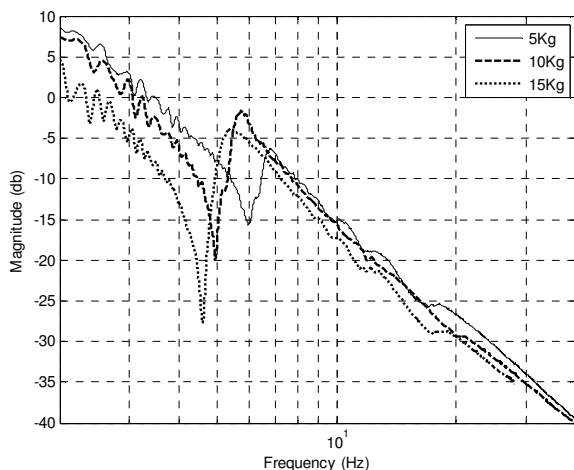


Fig. 14. Bode diagrams of the position to force response for 5 Kg, 10Kg and 15Kg loads.